

Fixed Electrical Charges and Mobile Ions Affect the Measurable Mechano-Electrochemical Properties of Charged-Hydrated Biological Tissues: The Articular Cartilage Paradigm

Leo Q. Wan¹, Chester Miller¹, X. Edward Guo², Van C. Mow^{1,3}

Abstract: The triphasic constitutive law [Lai, Hou and Mow (1991)] has been shown in some special 1D cases to successfully model the deformational and transport behaviors of charged-hydrated, porous-permeable, soft biological tissues, as typified by articular cartilage. Due to nonlinearities and other mathematical complexities of these equations, few problems for the deformation of such materials have ever been solved analytically. Using a perturbation procedure, we have linearized the triphasic equations with respect to a small imposed axial compressive strain, and obtained an equilibrium solution, as well as a short-time boundary layer solution for the mechano-electrochemical (MEC) fields for such a material under a 2D unconfined compression test. The present results show that the key physical parameter determining the deformational behaviors is the ratio of the perturbation of osmotic pressure to elastic stress, which leads to changes of the measurable elastic coefficients. From the short-time boundary layer solution, both the lateral expansion and the applied load are found to decrease with the square root of time. The predicted deformations, flow fields and stresses are consistent with the analysis of the short time and equilibrium biphasic (i.e., the solid matrix has no attached electric charges) [Armstrong, Lai and Mow (1984)]. These results provide a better understanding of the manner in which fixed electric charges and mobile ions within the tissue contribute to the observed material responses.

keyword: Articular Cartilage, Triphasic Theory, Unconfined Compression, Fixed Charge Density

1 Introduction

Articular cartilage is a thin layer of white, dense connective tissue covering the moving and load-supporting bony articulating ends in diarthrodial joints [Mow, Ratcliffe and Poole (1992)]. It is composed of an electrically charged and hydrated organic matrix of collagen and proteoglycan, where a sparse population of chondrocytes reside. Normal articular cartilage contains on average approximately 75% water within the pores of the tissue that are estimated to be 50-65 Å in diameter; even though its water content is high, its permeability is extremely low at approximately $10^{-15} m^4 / (N \cdot s)$ [ibid]. Figure 1 shows the organizational arrangement of the structural macromolecular components of the extracellular matrix of such tissue as articular cartilage [Heinegard, Bayliss and Lorenzo (2003)]. The most abundant components are collagen at about 10% per wet weight, followed by large aggregating proteoglycans at about 7.5% per wet weight [Mow and Ratcliffe (1997)]. Type II collagen is the dominant component of the collagen that exists in the tissue that also includes a number of quantitatively minor but functionally important collagen types, including V, VI, IX, and XI. Type II collagen fibers have an estimated half-life of 67 years, and they are capable of forming a strong meshwork of fine pores that traps proteoglycans in its intrafibrillar space. The quantitatively minor collagen types, particularly Type IX, are useful in facilitating interactions between the proteoglycans and collagen Type II fibers (Fig. 1). No covalent bonds exist between proteoglycans and the collagen meshwork; electrostatic interactions, frictional interactions and steric exclusion effects are responsible for immobilizing the large proteoglycans within the extracellular compartment of the tissue. Proteoglycans are architecturally complex macromolecules that are capable of forming networks in solution and within the interstitial fluid of the intrafibrillar space. Though labile these proteoglycan net-

¹ The Liu Ping Laboratory for Functional Tissue Engineering Research

² Bone Bioengineering Laboratory Department of Biomedical Engineering, Columbia University, New York, NY

³ Stanley Dicker Professor and Chair Department of Biomedical Engineering Columbia University, 351 Engineering Terrace 500 West 120th Street New York, NY 10027 Telephone: (212) 854-8462 Fax: (212) 854-8725 Email: vcml@columbia.edu

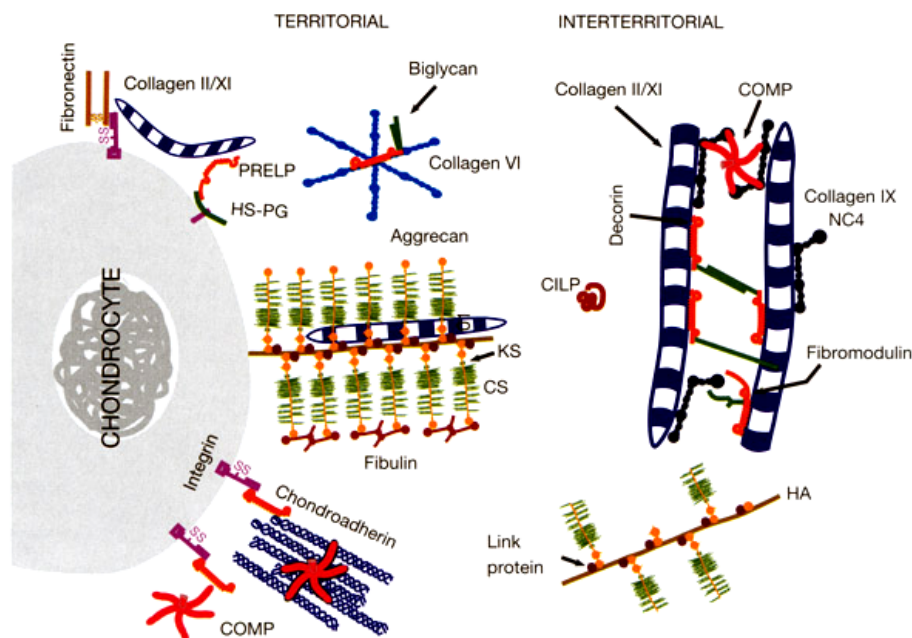


Figure 1 : The macromolecules of a cartilaginous extracellular matrix, their relationships with each other, and with chondrocytes. The structural load supporting macromolecules of articular cartilage are collagen of various types (II, V, VI, IX, XI) and the proteoglycans. Type II collagen phenotypically defines articular cartilage. Charges derived from carboxyl (COO^-) and sulfate (SO_4^{2-}) groups are fixed to the glycosaminoglycans attached to the protein cores of the proteoglycan. Other glycosaminoglycans include COMP, hyaluronan, fibromodulin, decorin, biglycan; these and others are organized in specific architectural arrangements for each specific connective tissue: articular cartilage, intervertebral disc, ligament, meniscus, tendon, etc [Heinegard, Bayliss and Lorenzo (2003)].

works can be deformed, and are viscoelastic and non-Newtonian [Mow, Zhu, Lai, Hardingham, Hughes and Muir (1989)]. Proteoglycans, hyaluronan, chondroadherin, COMP, heparin sulfate, fibronectin and integrin are attached to the chondrocyte surface via disulfide bonds and other non-specific attachment mechanisms (Fig. 1). These molecules are the antennae for the chondrocytes to sense the mechanical and electrochemical events occurring within the extracellular matrix when the tissue is loaded under *in vivo* conditions. An important objective for researchers in this field of study is to understand the mechanical and electrochemical events in the extracellular matrix in the immediate neighborhood of the cell. Normal tissues have a high negative fixed charged density (FCD); these negative charges are the carboxyl (COO^-) and sulfate (SO_4^{2-}) groups along with the glycosaminoglycans chains that are non-covalently attached to the protein cores of the proteoglycan macromolecules. Collagen and proteoglycans are the structural load support macromolecules comprising the solid matrix. The

FCD ranges from 0.5 \rightarrow 0.1 (or less) mEq/ml going from normal to diseased tissues, respectively [Maroudas (1979); Mow and Ratcliffe (1997)].

With traumatic injuries and diseases such as osteoarthritis, the collagen matrix of the porous-permeable matrix is irreversibly damaged and weakened, and there is a loss of the labile proteoglycan molecules. The simultaneous compositional changes in the cartilage solid matrix, *i.e.*, the increase of water content and decrease of FCD, and an alteration of electromechanical properties of the tissue, lead to inexorable changes in tissue deformational behaviors, less effective joint lubrication and load support mechanisms, and the eventual destruction of the joint [Mankin, Mow, Buckwalter, Iannotti and Ratcliffe (2000); Mow and Hung (2003)].

Biomechanically, articular cartilage plays an important role in providing a nearly frictionless, load-bearing, and shock-absorption surface between bones within a joint [Mow, Ratcliffe and Poole (1992); Mankin, Mow, Buckwalter, Iannotti and Ratcliffe (2000)]. To study the

mechano-electrochemical (MEC) properties of articular cartilage, and the interrelationships between the material properties and tissue composition, the unconfined compression test has been widely used in various experimental configurations, *e.g.* using either permeable or impermeable loading platens, and platens modeled with or without friction [Spilker, Suh and Mow (1990); Jurvelin, Buschmann and Hunziker (1997); Ateshian, Soltz, Mauck, Basalo, Hung and Lai (2003)]. This simple unconfined compression configuration has also been widely used in live-cartilage explants experiments for mechano-signal transduction studies and for various tissue engineering applications [Sah, Doong, Grodzinsky, Plaas and Sandy (1991); Kim, Sah, Grodzinsky, Plaas and Sandy (1994); Buschmann, Gluzband, Grodzinsky and Hunziker (1995); Mow, Wang and Hung (1999)]. Therefore, it is important to have a rigorous theory to extract valid mechanical and electrochemical properties of articular cartilage from unconfined compression experiments, to determine its MEC fields inside the tissue, and to correctly interpret results from live-explant studies so as to be able to deduce mechano-signal transduction mechanisms for chondrocytes [Mow, Wang, and Hung (1999)]. The tasks are facilitated by proper constitutive models for such biological tissues and full mathematical analyses of these problems.

Different constitutive material models, including such effects as compositional inhomogeneities and nonlinear permeability [Mow, Kuei, Lai, and Armstrong (1980); Lai, Mow, and Roth (1981)], transverse isotropy [Cohen, Lai and Mow (1998)], and matrix viscoelasticity and tension-compression nonlinearity models [Setton, Zhu, and Mow (1993); Soltz and Ateshian (2000); Huang, Soltz, Kopacz, Mow, and Ateshian (2003)] have been used to investigate the responses of articular cartilage under compression in the biomechanics literature. However, for this seemingly simple uniaxial loading (unconfined) compression test, daunting mathematical complexities have caused interpretative errors to occur in much of the biological and biochemical literatures studying cartilage tissue explants, and hence hinder rapid advances in our understanding of the mechano-signal transduction phenomenon. Therefore the overall aims of this paper are to provide additional insights into the MEC events within the tissue explant during unconfined compression, and to provide a set of simpler mathematical tools to facilitate analyses and interpretations of this important problem.

Armstrong, Lai and Mow (1984) were the first to analyze the unconfined compression problem of articular cartilage by using a linearized biphasic mixture theory introduced by Mow, Kuei, Lai and Armstrong (1980), in which the cartilage is assumed to consist of two phases: solid matrix and interstitial fluid. In the biphasic mixture theory, the solid matrix deformation is coupled with the interstitial fluid flow through the flow induced drag force. Since then, over the years, a series of problems were successfully solved for the biphasic theory under various loading and boundary conditions; these mathematical solutions gave a clearer understanding of tissue's mechanical and fluid transport behaviors, and the influence of interstitial fluid flow towards such mechanical behaviors as creep and stress relaxation [*e.g.*, see reviews by Mow, Ratcliffe and Poole (1992), and Mow and Ratcliffe (1997)]. These mathematical solutions have provided for the first time a detailed understanding of the interactive processes that occur between the porous-permeable solid matrix and the interstitial fluid during the unconfined compression experiment.

In the biphasic theory, however, the effects of the fixed negative charges of solid matrix are not explicitly considered, *i.e.*, where effects of charges (osmotic pressure) are lumped into the "apparent" mechanical parameters. The first analytical relationships between the fundamental physical parameters such as Faraday constant, diffusion coefficients, conductivity, absolute temperature, *etc.*, and the "apparent" mechanical parameters defining tissue permeabilities were given by Gu, Lai, and Mow (1993, 1998). In general, the observed changes are due to an excess of mobile ions accumulating in the charged interstitium when such tissues are bathed in an electrolyte solution; in this situation the FCD of the interstitium causes more counter-ions (Na^+) than co-ions (Cl^-) to enter the tissue than existing in the bathing solution. The colligative result of the imbalance of mobile ions is an excess of fluid pressure over the external fluid pressure; in other words, an osmotic swelling pressure or Donnan osmotic pressure [Maroudas (1979)]. It has long been conjectured that this osmotic pressure plays a dominant role in load support for articular cartilage.

To analytically model these electrochemical and osmotic swelling phenomena of articular cartilage from a continuum point of view, an additional phase (electrolyte ions) was included in the development of a tertiary mixture theory along with charges fixed to the solid porous-

permeable matrix; this was called the triphasic theory [Lai, Hou and Mow (1991)]. This new theory is entirely consistent with the biphasic theory, but it can explain more complex MEC events inside the tissue, such as solid matrix deformation, fluid flow, electrolyte transport, electrical potential, and swelling pressure [Gu, Lai and Mow (1998); Mow, Ateshian, Lai, Sun, Wang and Gu (1998); Lai, Mow, Sun and Ateshian (2000)]. A finite element formulation of triphasic theory was developed by Sun, Gu, Guo, Lai and Mow (1999) to study the effects of FCD on the unconfined compression behavior of articular cartilage [Sun, Mow, Lai and Guo (1999); Mow, Sun, Guo, Likhitanichkul and Lai (2002); Sun, Guo, Likhitanichkul, Lai and Mow (2004)]. Using the same finite element formulation, Lu, Sun, Guo, Chen, Lai and Mow (2004) successfully validated the predicted FCD by biochemical measurements, while simultaneously measuring the apparent mechanical properties from the indentation creep experiment. To date, however, these are the only triphasic results available. Moreover, these numerical solutions make it rather difficult, and time consuming, to determine MEC properties of articular cartilage from experiments such as unconfined compression or indentation, or to make general conclusions.

The primary objective, therefore, of this study is to develop an analytic solution for the unconfined compression response of the charged-hydrated, porous-permeable, soft tissue. This is to be accomplished by first linearizing the triphasic equations with respect to the imposed, infinitesimal compressive axial strain ϵ_0 , thereby rendering the governing equations analytically tractable. Thus, the specific aims of this paper are: a) to obtain the steady state equilibrium solution; and b) to analyze the short-time boundary layer behavior of the tissue following a Heaviside step load.

2 Methods

A schematic diagram for unconfined compression is shown in Fig. 2. A thin cylindrical wafer of cartilage sample with a radius of a and thickness h is placed in a saline solution of concentration c^* , and placed between two impermeable and frictionless platens. The tissue is compressed with a Heaviside step function of small compressive strain ϵ_0 along z axis. The radial expansion is unconstrained, and thus the fluid in the sample can flow freely in or out freely at the boundary $r = a$. The objective of the analysis is to describe the MEC fields in the

cartilage sample during the stress relaxation.

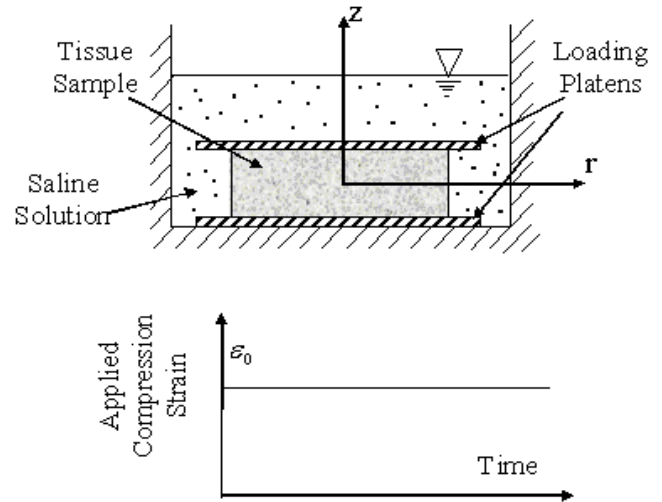


Figure 2 : Schematic of unconfined compression stress relaxation experiment for imposed Heaviside step displacement in the vertical direction between two frictionless platens.

2.1 Triphasic Formulations

Governing Equations

The governing equations for this problem are based on the triphasic theory [Lai, Hou, and Mow (1991); Gu, Lai, and Mow (1998)]. To simplify this problem, the cartilage sample is assumed to be homogenous and isotropic, and the solid matrix to be linearly elastic; also infinitesimal deformation theory is employed. The strain-dependent permeability effect and tension-compression nonlinearity are ignored so that we can focus on the effects of electrical charges.

The quasi-static momentum equations for the tissue, water, cation and anion are given by:

tissue

$$\nabla \cdot \boldsymbol{\sigma} = 0, \quad (1)$$

water

$$-\rho^w \nabla \mu^w + f_{ws}(\mathbf{v}^s - \mathbf{v}^w) + f_{w+}(\mathbf{v}^+ - \mathbf{v}^w) + f_{w-}(\mathbf{v}^- - \mathbf{v}^w) = 0, \quad (2)$$

cation

$$-\rho^+ \nabla \tilde{\mu}^+ + f_{+w}(\mathbf{v}^w - \mathbf{v}^+) = 0, \quad (3)$$

anion

$$-\rho^- \nabla \tilde{\mu}^- + f_{-w}(\mathbf{v}^w - \mathbf{v}^-) = 0, \quad (4)$$

where, $\boldsymbol{\sigma}$ is the total stress acting in the tissue; μ^w , $\tilde{\mu}^+$ and $\tilde{\mu}^-$ are the chemical potential for water and electrochemical potentials for cations and anions, respectively. The term ρ^α (w stands for water, $+$ for cations, and $-$ for anions) is the apparent density of phase α , and \mathbf{v}^α is its velocity. The densities ρ^α are related to water volume fraction ϕ^w and ion concentration c^α by:

$$\rho^w = \rho_T^w \phi^w, \quad \rho^+ = \phi^w c^+ M_+, \quad \rho^- = \phi^w c^- M_-, \quad (5)$$

where ρ_T^w is the true density of water phase, M_α is the α -ion molecular weight. The coefficients $f_{\alpha\beta}$ are the diffusive drag coefficients between phases α and β , and the reciprocity $f_{\alpha\beta} = f_{\beta\alpha}$ relationship is assumed. They are related to interstitial fluid permeability k and ion diffusivities D^+ and D^- through the following relationships:

$$k = \frac{\phi^{w^2}}{f_{ws}}, \quad D^+ = \frac{\phi^w R T c^+}{f_{w+}}, \quad D^- = \frac{\phi^w R T c^-}{f_{w-}} \quad (6)$$

where R is the universal gas constant and T is the absolute temperature [Gu, Lai, and Mow (1998)]. The drag forces between cations and anions, and between ions and solid matrix have been neglected from the momentum equations.

The constitutive equations for the total stress $\boldsymbol{\sigma}$, chemical potential for water (μ^w) and electrochemical potentials for cations ($\tilde{\mu}^+$) and anions ($\tilde{\mu}^-$) are given by:

tissue

$$\boldsymbol{\sigma} = -p\mathbf{I} + \lambda_s e \mathbf{I} + 2\mu_s \mathbf{E}, \quad (7)$$

water

$$\mu^w = \mu_0^w + [p - RT\phi(c^+ + c^-)]/\rho_T^w, \quad (8)$$

cation

$$\tilde{\mu}^+ = \mu_0^+ + (RT/M_+) \ln(\gamma_+ c^+) + F_c \Psi / M_+, \quad (9)$$

anion

$$\tilde{\mu}^- = \mu_0^- + (RT/M_-) \ln(\gamma_- c^-) - F_c \Psi / M_-, \quad (10)$$

where λ_s and μ_s are the intrinsic Lamé's constants for the elastic solid matrix. The strain tensor \mathbf{E} is for small strains of the solid phase, and e is its trace, also known as the dilatation of solid matrix. The term p is the interstitial fluid pressure, ϕ is the osmotic coefficient, γ_+ and γ_- are the activity coefficients of the ions, F_c is the Faraday's constant, and Ψ is the electric potential inside the tissue.

The continuity equations for different phases are given by:

$$\frac{\partial \rho^\alpha}{\partial t} + \nabla \cdot (\rho^\alpha \mathbf{v}^\alpha) = 0. \quad (11)$$

We used the condition of intrinsic incompressibility for both the solid phase and the fluid phase of cartilage [Bachrach, Guilak, and Mow (1998)], and neglected the volume of cations and anions, therefore, the continuity equation of the mixture is:

$$\nabla \cdot (\phi^s \mathbf{v}^s + \phi^w \mathbf{v}^w) = 0 \quad (12)$$

The electroneutrality condition is given by:

$$c^+ = c^- + c^F, \quad (13)$$

where c^F is the negative charge density of the solid matrix.

The FCD (designated as c^F in the governing equations) of the solid matrix changes as the matrix solid is deformed according to the equation:

$$c^F = c_0^F / \left(1 + \frac{e}{\phi_0^w}\right), \quad (14)$$

where c_0^F and ϕ_0^w are the fixed charge density and porosity of the tissue at the reference state, respectively.

Since the interface between the cylindrical sample and platens is assumed to be perfectly smooth (*i.e.*, frictionless) the deformation should be independent of z [Armstrong, Lai, and Mow (1984)]. Therefore, this axisymmetric problem becomes, spatially, a one-dimensional problem with respect to the radial coordinate r . All dependent variables will be functions only of r and t , and the principal directions of stress and strain will align with the radial, circumferential, and axial directions of the sample. The entire process can be divided into two stages: 1) an instantaneous isochoric deformation resulting from the imposed compression at $t = 0^+$, and 2) a stress relaxation period from $t = 0^+$ to $t \rightarrow \infty$, in

Table 1 : Essential parameters at reference state

Parameters	c_0^+	c_0^-	p_0	ψ_0
Reference state value	$\frac{c_0^F + c_0^k}{2}$	$\frac{-c_0^F + c_0^k}{2}$	$\phi RT(c_0^k - 2c^*)$	$\frac{RT}{F_c} \ln\left(\frac{-c_0^F + c_0^k}{2c^*}\right)$

which the sample continues to deform radially (expanding initially, and contracting toward equilibrium for intrinsic Poisson’s ratio less than 0.5). From the standpoint of investigating of the stress relaxation of articular cartilage, the instantaneous response (stage 1) provides the initial condition.

Reference State

Prior to compression, the tissue is equilibrated in a saline solution containing a univalent electrolyte of concentration of c^* . The chemical potential for water μ^w and electrochemical potential for cations $\tilde{\mu}^+$ and anions $\tilde{\mu}^-$ are uniform both inside and outside of the tissue, which, together with outside hydraulic pressure p , are often normalized to be zero. Since these potentials within the external saline solution are held constant with time, the parameters could be set equal to zero throughout the unconfined compression stress-relaxation process. In this paper, this free swollen state is chosen as a reference to study the change of physical parameters. The values of the dependent variables at reference state are given in Tab. 1, in which c_0^k is the sum of ion concentration at the reference state and given by:

$$c_0^k = c_0^+ + c_0^- = \sqrt{4 \frac{\gamma_+^* \gamma_-^*}{\gamma_+ \gamma_-} (c^*)^2 + (c_0^F)^2} \quad (15)$$

Boundary Condition

At the lateral edge just inside the tissue,

$$\mu^w = \mu^{w*}, \quad \tilde{\mu}^+ = \tilde{\mu}^{+*} \quad \text{and} \quad \tilde{\mu}^- = \tilde{\mu}^{-*} \quad \text{at} \quad r = a^- \quad (16a)$$

$$\sigma_{rr} = 0 \quad \text{at} \quad r = a^- \quad (16b)$$

where, μ^{w*} , $\tilde{\mu}^{+*}$ and $\tilde{\mu}^{-*}$ are chemical potential for water and electrochemical potentials for cations and anions in the saline solution, respectively. They are assumed to be constant throughout the entire process.

At the center of the tissue, the solid matrix is assumed to have no radial displacement and flux of water, cations and anions must be zero according to the symmetric condition, *i.e.* [Sun, Guo, Likhitpanichkul, Lai and Mow (2004)].

$$u_r = 0, \quad \phi^w (v_r^w - v_r^s) = 0, \quad \phi^w c^+ (v_r^+ - v_r^s) = 0, \quad \phi^w c^- (v_r^- - v_r^s) = 0 \quad (17)$$

2.2 Methods of Solution

Since the imposed compressive strain ϵ_o is a small parameter, the “perturbation method” can be used to find the analytic solution [Sun, Guo, Likhitpanichkul, Lai and Mow (2004)]. Using the regular perturbation sequence for the unknowns such as c^F, ψ, e and $\tilde{\mu}$,

$$Q = Q_0 + \epsilon_0 Q_1 + \epsilon_0^2 Q_2 + \dots, \quad (18)$$

where Q_0 is the value at reference state, and $\delta Q = Q - Q_0 \approx \epsilon_0 Q_1$ is its linearized perturbation, constitutive equations (7)-(10) will become:

$$\delta \sigma_{zz} = -\delta p + \lambda_s \delta e - 2\mu_s \epsilon_0, \quad (19a)$$

$$\delta \sigma_{rr} = -\delta p + \lambda_s \delta e + 2\mu_s \frac{\partial u_r}{\partial r}, \quad (19b)$$

$$\delta \sigma_{\theta\theta} = -\delta p + \lambda_s \delta e + 2\mu_s \frac{u_r}{r}, \quad (19c)$$

$$\delta \mu^w = \delta p - \phi RT \delta c^k, \quad (20)$$

$$\delta \tilde{\mu}^+ = \frac{RT}{M^+} \frac{\delta c^+}{c_0^+} + \frac{F_c}{M^+} \delta \psi, \quad (21)$$

$$\delta \tilde{\mu}^- = \frac{RT}{M^-} \frac{\delta c^-}{c_0^-} - \frac{F_c}{M^-} \delta \psi, \quad (22)$$

Here, the perturbation to the dilatation is given by:

$$\delta e = \frac{\partial u}{\partial r} + \frac{u}{r} - \epsilon_o \quad (19d)$$

Table 2 : Essential parameters at initial state and steady state

	Initial state		Steady state
	interior	Edge	
λ	1/2	$\frac{1}{4(1-\nu_A)}$	ν_A
e	0	$-\frac{1-2\nu_A}{2(1-\nu_A)}\epsilon_0$	$-(1-2\nu_A)\epsilon_0$
δc^F	0	$\frac{c_0^F}{\phi_0^w} \frac{1-2\nu_A}{2(1-\nu_A)}\epsilon_0$	$\frac{c_0^F}{\phi_0^w} (1-2\nu_A)\epsilon_0$
δc^k	0	$\frac{H_a}{RT} \frac{\nu_A - \nu_s}{2(1-\nu_s)(1-\nu_A)}\epsilon_0$	$\frac{H_a}{RT} \frac{\nu_A - \nu_s}{1-\nu_s}\epsilon_0$
δp	$\mu_s \epsilon_0$	$H_a \frac{\nu_A - \nu_s}{2(1-\nu_s)(1-\nu_A)}\epsilon_0$	$H_a \frac{\nu_A - \nu_s}{1-\nu_s}\epsilon_0$
$\delta \sigma_{zz}$	$3\mu_s \epsilon_0$	$-2\mu_s \frac{2-\nu_A}{1-\nu_A}\epsilon_0$	$-2\mu_s(1+\nu_A)\epsilon_0$
$\delta \psi$	$* \delta \psi_{0i}$	$-\frac{H_a}{F_c c_o^F} \frac{\nu_A - \nu_s}{2(1-\nu_s)(1-\nu_A)}\epsilon_0$	$-\frac{H_a}{F_c c_o^F} \frac{\nu_A - \nu_s}{1-\nu_s}\epsilon_0$

$$* \delta \psi_{0i} = \delta \psi_{0E} + \frac{2H_a \epsilon_0}{c_o^F F_c} \left(c_3 \left(-1 + \frac{1}{q_1} \right) + c_4 \left(-1 + \frac{1}{q_2} \right) \right)$$

2.3 Steady State Analysis

After the application of the Heaviside function for the imposed strain (ϵ_0) the tissue will experience stress relaxation that will eventually reach equilibrium when all flow processes cease. Therefore, according to momentum equations (2-4), the chemical potential of water and electrochemical potentials of ions inside the tissue will be equal to those in the external saline solution. Since the potentials of three phases outside the tissue are assumed to be constant (zero), we have:

$$\delta \mu^w = 0, \quad \delta \tilde{\mu}^+ = 0, \quad \delta \tilde{\mu}^- = 0. \quad (23)$$

Based on the momentum equation for the overall tissue (Eq. (1)), the tissue can be treated as an elastic body, and the total stress must satisfy:

$$\delta \sigma_{rr} = 0, \quad \delta \sigma_{\theta\theta} = 0. \quad (24)$$

From Eqs. (19)-(24), we can solve for the equilibrium apparent Poisson's ratio ν_A and the equilibrium apparent Young's modulus E_A (see Appendix A),

$$\nu_A = \frac{\nu_s + (1 - \nu_s)\xi}{1 + 2(1 - \nu_s)\xi}, \quad (25)$$

$$E_A = \frac{\delta \sigma_{zz}}{-\epsilon_0} = 2\mu_s(1 + \nu_A) = E_s \frac{1 + \nu_A}{1 + \nu_s}, \quad (26)$$

where ν_s is the (intrinsic) Poisson's ratio of solid matrix, and

$$\xi = M/f \quad (27)$$

with $f = c_0^k/c_0^F$ and M is a dimensionless number which we defined as ‘‘Mechano-electrochemical (MEC) number’’ given by:

$$M = \frac{\phi RT c_0^F}{\phi_0^w H_a}. \quad (28)$$

Physically, the MEC number represents the ratio of the electrostatic force to the mechanical force generated in the solid matrix due to deformation. The parameter ξ is similar to that found in reference by Ateshian, Chahine, Basalo and Hung (2004). The perturbation of other parameters at the final steady state can be expressed in terms of ν_A and given in Tab. 2.

2.4 Time-Dependent Analysis

As stated above, the unconfined compression problem is spatially a one-dimensional problem in r . By making use of the perturbation method, and neglecting terms second or higher order in the imposed compressive strain (*e.g.*, advection terms), we have been able to reduce the number of dependent variables and partial differential equa-

tions (PDEs) in the analysis from 4 to just 2 – see Appendix B, and reference [Sun, Guo, Likhitanichkul, Lai and Mow (2004)].

In order to simplify this problem, the following dimensionless parameters are introduced:

$$\hat{r} = \frac{r}{a}, \quad \hat{u}_r = \frac{u_r}{a}, \quad \hat{t} = \frac{D^B}{a^2}t, \quad \hat{D}^+ = \frac{D^+}{D^B},$$

$$\hat{D}^- = \frac{D^-}{D^B}, \quad \hat{c} = \frac{RTc}{H_a}. \quad (29)$$

The two dimensionless dependent variables employed in the present analysis are the apparent Poisson's ratio λ and dimensionless overall ionic concentration γ . Both variables depend on time and radial point (\hat{t} , \hat{r}), and are defined by the following equations:

$$\lambda = \frac{1}{2\varepsilon_0} \left(\hat{r} \frac{\partial \hat{u}_r}{\partial \hat{r}} + \hat{u}_r \right), \quad \text{and} \quad \gamma = \frac{\delta c^k}{2\varepsilon_0}. \quad (30)$$

As derived in Appendix B, these new dependent variables satisfy the following two PDEs:

$$\frac{1}{\hat{r}} \frac{\partial}{\partial \hat{r}} \left(\hat{r} \frac{\partial \lambda}{\partial \hat{r}} \right) = B_{11} \frac{\partial \lambda}{\partial \hat{t}} + B_{12} \frac{\partial \gamma}{\partial \hat{t}}, \quad (31a)$$

$$\frac{1}{\hat{r}} \frac{\partial}{\partial \hat{r}} \left(\hat{r} \frac{\partial \gamma}{\partial \hat{r}} \right) = B_{21} \frac{\partial \lambda}{\partial \hat{t}} + B_{22} \frac{\partial \gamma}{\partial \hat{t}}, \quad (31b)$$

where B_{11} , B_{12} , B_{21} and B_{22} are given in the list of Nomenclature at the end of the manuscript. These equations are much simpler in mathematical form than the general non-linear equations [Sun, Guo, Likhitanichkul, Lai and Mow (2004)] and resemble the familiar relationships encountered in simple transient diffusion problems [Carslaw and Jaeger (1959)].

Boundary Conditions

The boundary conditions for Eqs. (31) in the new dependent variables (λ , γ) become:

$$\hat{r} \frac{\partial \lambda}{\partial \hat{r}} \rightarrow 0, \quad \text{at} \quad \hat{r} \rightarrow 0 \quad \text{all} \quad \hat{t} > 0, \quad (32a)$$

$$\hat{r} \frac{\partial \gamma}{\partial \hat{r}} \rightarrow 0, \quad \text{at} \quad \hat{r} \rightarrow 0 \quad \text{all} \quad \hat{t} > 0, \quad (32b)$$

$$\frac{2(1-\nu_A)}{(1-2\nu_A)}\lambda - 2 \int_0^1 \hat{r}' \lambda d\hat{r}' = \frac{\nu_A}{(1-2\nu_A)}$$

at $\hat{r} = 1$ all $t > 0$, (32c)

$$\gamma = \frac{(\nu_A - \nu_s)(1-2\lambda)}{2(1-\nu_s)(1-2\nu_A)} \quad \text{at} \quad \hat{r} = 1 \quad \text{all} \quad \hat{t} > 0. \quad (32d)$$

The first two boundary conditions indicate that there is no radial flux of ions at the center of the sample (Eq.17). The third is derived from the combination of conditions that, at the radial edge of the sample, a) the chemical potential of water must match the value in the bathing solution, and b) the radial component of the total stress tensor must equal zero. The last equation follows the condition that the chemical potentials of the positive and negative ions are continuous at the radial edge of the sample.

Initial Conditions

As indicated in Sun, Guo, Likhitanichkul, Lai and Mow (2004), the tissue will experience an instantaneous isochoric deformation at time zero (*i.e.*, the volume of tissue will remain constant with no efflux of water). Throughout the entire mass of tissue sample (with the exception of a boundary layer at the edge) the transient Poisson's ratio will therefore be equal to 0.5 initially. The initial conditions for the partial differential governing equations, *i.e.*, Eqs. (31), are thus

$$\lambda = 1/2, \quad \text{at} \quad \hat{t} = 0 \quad \text{all} \quad \hat{r} < 1. \quad (33a)$$

$$\gamma = 0, \quad \text{at} \quad \hat{t} = 0 \quad \text{all} \quad \hat{r} < 1. \quad (33b)$$

2.5 Similarity Solutions for the Boundary Layer

For short dimensionless times (with respect to the gel diffusion time $\tau_g = a^2/(Hak)$), the mathematical solution for Eqs. (31) will exhibit boundary layer behavior in the vicinity of $\hat{r} = 1$. This means that the dependent variables will vary rapidly with radial position near the boundary, but in the interior of the domain the dependent variables will slowly evolve with time. With respect to the radius, the monotonically decreasing nature of the γ and λ will not change until they reach an equilibrium constant value.

For numerical solutions (*e.g.*, finite element method), it is difficult to obtain accurate numerical results for the sharp spatial variations of the dependent variables, particularly near the boundary $\hat{r} = 1$, where these parameters vary very rapidly with radial position unless a large number of discretized elements are used near the boundary. In order to overcome this difficulty, particularly at short times, we

have developed a special asymptotic analytic approximation for the limit of short times.

For positions very near the edge, the curvature of the specimen may be neglected, the cylindrical coordinates will be reduced to Cartesian coordinates, and hence by introducing a similarity variable ζ

$$\zeta = \frac{x}{2\sqrt{\hat{t}}} = \frac{1-\hat{r}}{2\sqrt{\hat{t}}} \quad (34)$$

in Eq. (31), we transform the two PDEs into two coupled ordinary differential equations (ODEs),

$$\frac{d^2\lambda}{d\zeta^2} = -2\zeta \left(B_{11} \frac{d\lambda}{d\zeta} + B_{12} \frac{d\gamma}{d\zeta} \right), \quad (35a)$$

$$\frac{d^2\gamma}{d\zeta^2} = -2\zeta \left(B_{21} \frac{d\lambda}{d\zeta} + B_{22} \frac{d\gamma}{d\zeta} \right). \quad (35b)$$

From the initial condition (33), we have boundary conditions:

$$\lambda \rightarrow 1/2, \quad \gamma \rightarrow 0 \quad \text{at} \quad \zeta \rightarrow \infty. \quad (36)$$

Considering that the integral on the left hand side of Eq. (32c) is dominated by the far field value of λ (*i.e.*, $\lambda = 1/2$) during the boundary layer development, the boundary conditions Eq. (32c) and Eq. (32d) become:

$$\lambda = \lambda^* = \frac{1}{4(1-\nu_A)} \quad \text{at} \quad \zeta = 0, \quad (37a)$$

$$\gamma = \gamma^* = \frac{1}{4(1-\nu_A)} - \frac{1}{4(1-\nu_s)} \quad \text{at} \quad \zeta = 0. \quad (37b)$$

The mathematical solutions of the coupled ODEs, with corresponding boundary conditions are:

$$\left(\lambda - \frac{1}{2} \right) = - (C_3 \operatorname{erfc}(\sqrt{q_1}\zeta) + C_4 \operatorname{erfc}(\sqrt{q_2}\zeta)), \quad (38a)$$

$$\left(\gamma - \frac{1}{2} \right) = \frac{B_{21}}{P_1} C_3 \operatorname{erfc}(\sqrt{q_1}\zeta) - \frac{P_1}{B_{12}} C_4 \operatorname{erfc}(\sqrt{q_2}\zeta), \quad (38b)$$

where *erfc* represents the complimentary error function. The parameters B_{12} , $B_{21}P_1$, q_1 , q_2 , C_3 and C_4 are given in the list of Nomenclature.

At the initial state, *i.e.*, $t = 0^+$, the dependent variables are listed in Tab. 2 for the interior, and at the edge $\hat{r} = 1^-$. The initial values at the edge of the tissue are calculated according to the boundary condition Eq. (37a) and the continuity of the water, anion and cation potentials (Eqs. 23). The variables in the interior of the tissue are evaluated based on the initial isochoric solution, or by integrating across the boundary layer.

2.6 Derivation of Experimentally Measurable Variables

Among the variables listed in Tab. 2, only a small fraction have typically been measured experimentally to determine the biomechanical and biochemical properties of such charged-hydrated tissues. These include: a) the lateral expansion; b) the applied load; and c) the electrical potential [Gu, Lai and Mow (1993); Jurvelin, Buschmann and Hunziker (1997); Wong, Ponticciello, Kovanen and Jurvelin (2000); Garon, Legare, Guardo, Savard and Buschmann (2002)].

During the stress relaxation process occurring in the unconfined compression test, and for short times, the lateral expansion may be obtained by integrating the mathematical solution for λ :

$$u_E = \hat{u}_E a = a \int_0^1 2\lambda \varepsilon_0 \hat{r} d\hat{r} = \bar{\lambda} a \varepsilon_0. \quad (39)$$

The force acting on the end faces of the cylindrical specimen may be obtained by using Eq. (19a) and radially integrating Eq. (B9):

$$F = - \int_0^1 2\pi \hat{r} \sigma_{zz} d\hat{r} = -2\pi a^2 \varepsilon_0 \mu_s (1 + \bar{\lambda}). \quad (40)$$

Here, $\bar{\lambda}$ is the area average of the short time solution for the Poisson's ratio given by:

$$\bar{\lambda} = 2 \int_0^1 \hat{r} \lambda d\hat{r} = \frac{1}{2} - 4 \left(\frac{C_3}{\sqrt{q_1}} + \frac{C_4}{\sqrt{q_2}} \right) \sqrt{\frac{\hat{t}}{\pi}}. \quad (41)$$

This mathematical solution may be simplified for the special case where diffusivities of the cations and anions are the same, *i.e.*, $D^d = 0$. In this case, the above solution for the area average Poisson's ratio becomes:

$$\bar{\lambda} = \frac{1}{2} - \frac{1-2\nu_A}{1-\nu_A} \sqrt{\frac{\hat{t}}{q_1 \pi}}, \quad \text{or} \quad \bar{\lambda} = \frac{1}{2} - \frac{1-2\nu_A}{1-\nu_A} \sqrt{\frac{H_a k t}{q_1 \pi a^2}}, \quad (42a)$$

Table 3 : Range of the parameters of articular cartilage and the base case

	FCD (mEq/ml)	Porosity	Intrinsic Poisson's Ratio	Intrinsic Aggregate Modulus H_a (MPa)	Permeability k ($\times 10^{-15} \text{ m}^4/(\text{N}\cdot\text{s})$)
Range	0.01-0.5	0.7-0.85	0.0-0.4	0.2-1.0	0.4-5
Base case	0.2	0.75	0.2	0.4	1.07

where q_1 will be simplified:

$$q_1 = \frac{\hat{D}^a(1 + \xi)}{\hat{D}^a + \xi}, \quad \text{or} \quad q_1 = \frac{D^a(1 + \xi)}{D^a + H_a k \xi}. \quad (42b)$$

Solution Eqs. (42a) shows the \sqrt{t} decaying behavior of the lateral expansion (and the force relaxation as well). If we further assume that as the fixed charge density approaches zero, the non-dimensional parameter $\xi \rightarrow 0$, and thus the triphasic problem will be reduced to the biphasic problem with $v_A = v_s$ and $q_1 = 1$. Under these circumstances, Eqs. (42) become:

$$\bar{\lambda} = \frac{1}{2} - \frac{1 - 2v_s}{1 - v_s} \sqrt{\frac{\hat{t}}{\pi}}, \quad \text{or} \quad \bar{\lambda} = \frac{1}{2} - \frac{1 - 2v_s}{1 - v_s} \sqrt{\frac{H_a k t}{\pi a^2}}. \quad (43)$$

Now, by substituting $\bar{\lambda}$ into Eqs. (39) and (40), we obtain the relaxation behavior of the lateral expansion and the applied load at short dimensionless times for the case $FCD \rightarrow 0$. (See paper by Armstrong, Lai and Mow (1984) for the mathematical solution of the biphasic unconfined compression problem.)

The electrical potential response at short times can be obtained by inserting the dilatation e into Eqs. (B12):

$$\delta\psi = \delta\psi_E + \frac{2H_a \epsilon_0}{c_0^F F_c} \left(C_3 \text{erf}(\sqrt{q_1} \zeta) \left(-1 + \frac{1}{q_1} \right) + C_4 \text{erf}(\sqrt{q_2} \zeta) \left(-1 + \frac{1}{q_2} \right) \right), \quad (44a)$$

where, erf represents the error function, and $\delta\psi_E$ is the electrical potential history at $\hat{t} = 1^-$ relative to the external solution, which is given by:

$$\delta\psi_E = -\frac{c_0^F RT}{c_0^k F_c \phi_0^w} (1 - 2\lambda_E) \epsilon_0. \quad (44b)$$

The initial value of electric potential perturbation in the interior ($\delta\psi_{0i}$) is obtained by substituting $\zeta \rightarrow \infty$ into the

equation above,

$$\delta\psi_{0i} = \delta\psi_{0E} + \frac{2H_a \epsilon_0}{c_0^F F_c} \left(C_3 \left(-1 + \frac{1}{q_1} \right) + C_4 \left(-1 + \frac{1}{q_2} \right) \right), \quad (45)$$

where $\delta\psi_{0E}$ is the initial value of electrical potential perturbation at the edge, and given in Tab. 2.

3 Numerical Results

Using the intrinsic properties of the tissue and the parameters of surrounding electrolyte solution, it is now possible to determine numerically the lateral expansion, tissue load response at the surface, and the electrical potential for both the steady state and short dimensionless times. For this purpose, we introduce a ‘‘base case’’ defined by a set of realistic and physiologically normal values for the intrinsic parameters of the tissue as listed in Tab. 3. These were selected to be identical to those considered in the finite element solution in the reference by Sun, Guo, Likhitanichkul, Lai and Mow (2004). The radius of the specimen was taken to be 1.5 mm. For the electrolyte, the following base case parameters are used: $\phi = 1$, $\gamma_+^* \gamma_-^* / \gamma_+ \gamma_- = 1$, $c^* = 0.15M$, $D^+ = 0.5 \times 10^{-9} \text{ m}^2/\text{s}$ and $D^- = 0.8 \times 10^{-9} \text{ m}^2/\text{s}$. We note that ξ , the ratio of the parameter $M = RT c_0^F / (\phi_0^w H_a)$ to the parameter $f = c_0^k / c_0^F$, is a dimensionless parameter describing the ratio of osmotic pressure change and elastic stress change due to small deformations within the tissue. At 20°C , the typical range of values for M is expected to be on the order of $10^{-3} - 10^1$, and ξ is on the order of $10^{-5} - 10^1$ (Tab. 3). Therefore, for the base case, M and ξ are about 1.6 and 0.9, respectively, and the variations $f = c_0^k / c_0^F$ and ξ with FCD for different external solution concentrations are presented in Figs. 3 and 4, respectively.

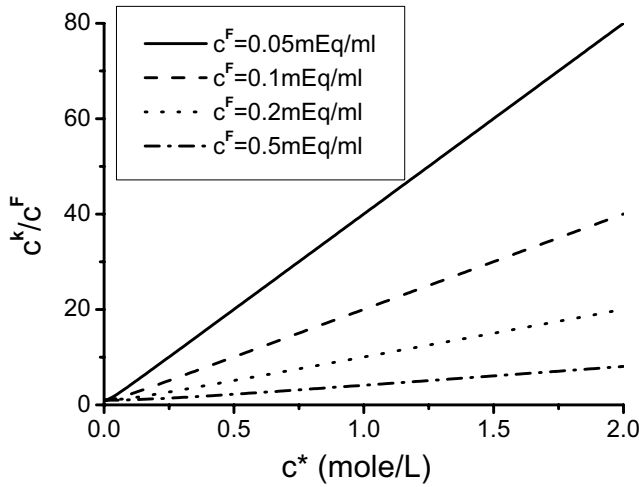


Figure 3 : Ratio of c^k/c^F as a function of external ion concentration c^* for various values of fixed charge density c^F . ($c^k/c^F = \sqrt{4(c^*/c^F)^2 + 1}$; $c^k = c^+ + c^-$)

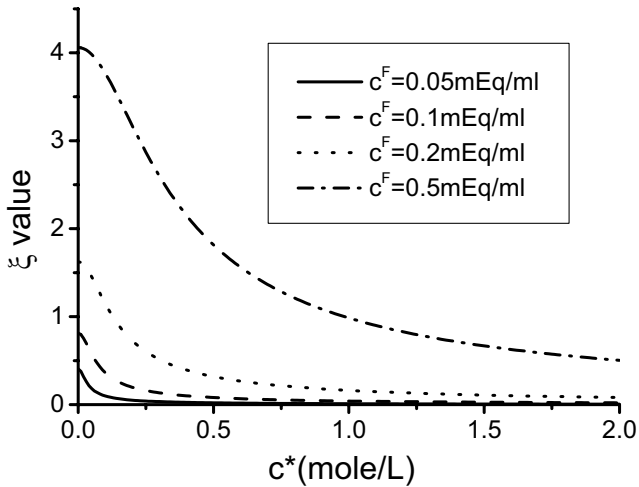


Figure 4 : Variation of ξ with external ion concentration c^* for various values of tissue fixed charge density c_o^F in base case: osmotic coefficient $\phi = 1$, absolute temperature $T = 293.15K$, porosity $\phi_0^w = 0.75$, aggregate modulus $H_a = 0.4Mpa$. ($\xi = M/f$ with $M = \phi RT c_o^F / (\phi_0^w H_a)$ and $f = \sqrt{4(c^*/c_o^F)^2 + 1}$)

3.1 Steady State Analysis

Equation (25) shows that the variation of the equilibrium apparent Poisson's ratio v_A with intrinsic Poisson's ratio v_s depends solely and simply on the parameter ξ , Fig.

5. From Figs. 4 and 5, we can observe that for the low FCD case (e.g., in the pathological state $\sim 0.01mEq/ml$), the parameter ξ is relatively small, and thus the equilibrium apparent Poisson's ratio v_A is close to the intrinsic Poisson's ratio v_s . On the other hand, if the FCD is high (e.g., in the normal physiological range $\sim 0.5 mEq/ml$), ξ will be large (Fig. 4), and thus the overall tissue will be relatively incompressible (Fig. 5).

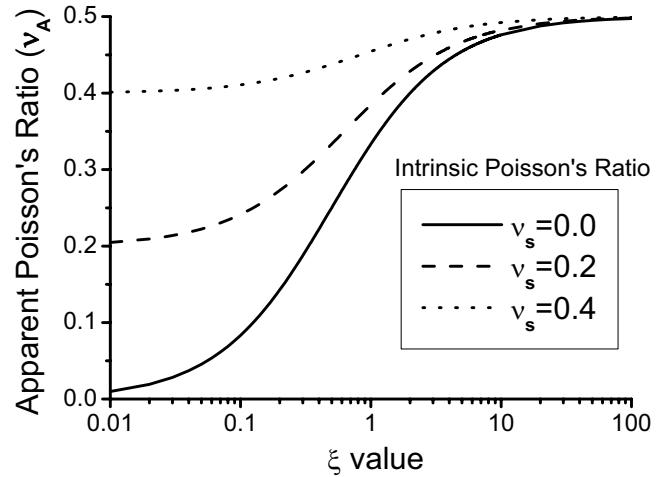


Figure 5 : Variation of equilibrium apparent Poisson's ratio with ξ for range of intrinsic Poisson's ratios. ($v_A = \frac{v_s + (1-v_s)\xi}{1 + 2(1-v_s)\xi}$ where $\xi = M/f$ with $M = \phi RT c_o^F / (\phi_0^w H_a)$ and $f = \sqrt{4(c^*/c_o^F)^2 + 1}$.)

At steady state, Figs. 6 and 7 show the ratio of the apparent Young's modulus (E_A) to intrinsic Young's modulus (E_s) and electrical potential difference between the equilibrium state ψ_∞ and the reference state ψ_0 , respectively, as a function of ξ , for different values of the intrinsic Poisson's ratio. Measurement of the equilibrium load required to compress the tissue following stress relaxation, and measurement of the difference between the initial and equilibrium electric potentials (relative to the electrolyte bathing solution) provides two additional equations to solve for the elastic and electromechanical parameters defining charged-hydrated solid matrix. From Fig. 7 and the expression of the electrical potential perturbation in Tab. 2, we can conclude that $H_a \epsilon_0 \geq -2F_c c_o^F \delta\psi_\infty$, regardless of the values for the intrinsic Poisson's ratio and the external solution concentration. For the base case, $-10.4mv \leq \delta\psi_\infty / \epsilon_0 < 0$.

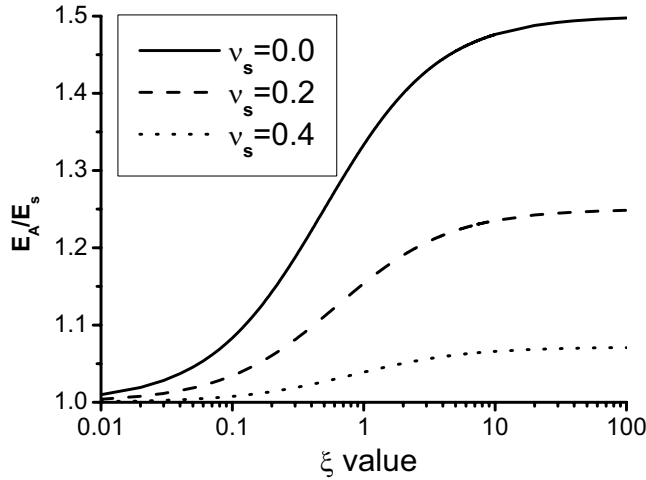


Figure 6 : Variation of the normalized apparent Young's modulus E_A with ξ for a range of intrinsic Poisson's ratios. E_A and E_s are the apparent Young's modulus and intrinsic Young's modulus, respectively. ($\frac{E_A}{E_s} = \frac{\delta\sigma_{zz}}{-E_s\epsilon_0} = \frac{1+v_A}{1+v_s}$, where $v_A = \frac{v_s+(1-v_s)\xi}{1+2(1-v_s)\xi}$ and $\xi = M/f$, with $M = \phi RT c_0^F / (\phi_0^w H_a)$ and $f = \sqrt{4(c^*/c_0^F)^2 + 1}$)

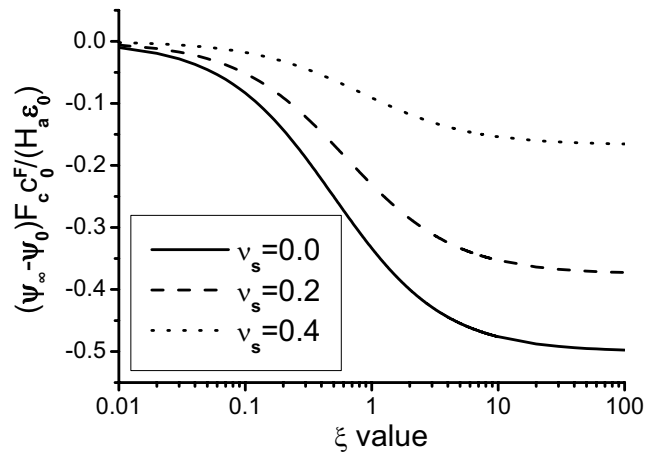


Figure 7 : Variation of steady state electrical potential perturbation $(\delta\psi)$ with ξ for different values of intrinsic Poisson's ratio v_s . ($\frac{(\psi_\infty - \psi_0) F_c c_0^F}{H_a \epsilon_0} = -\frac{v_A - v_s}{1 - v_s}$ where, $v_A = \frac{v_s+(1-v_s)\xi}{1+2(1-v_s)\xi}$ and $\xi = M/f$, with $M = \phi RT c_0^F / (\phi_0^w H_a)$ and $f = \sqrt{4(c^*/c_0^F)^2 + 1}$)

3.2 Time Dependent Solution

The short time histories of the lateral expansion of the tissue and the applied load are given in Eqs. (39) and (40),

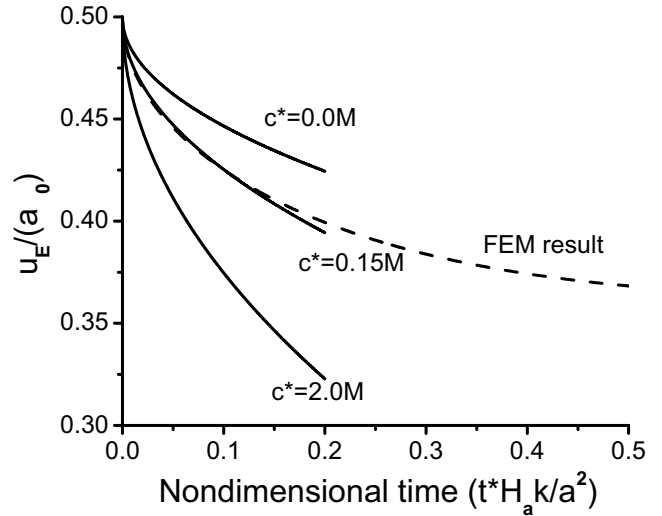


Figure 8 : Predicted short time history of the normalized lateral expansion u_E for a range of external saline concentrations (also shown the numerical FEM full time-dependent result). (Base case: osmotic coefficient $\phi = 1$, absolute temperature $T = 293.15K$, external ionic concentration $c^* = 0.15M$, fixed charge density $c_0^F = 0.15mEq/ml$, cation diffusivity $D^+ = 0.5 \times 10^{-9}m^2/s$, anion diffusivity $D^- = 0.8 \times 10^{-9}m^2/s$, applied strain $\epsilon_0 = 0.1$, porosity $\phi_0^w = 0.75$, aggregate modulus $H_a = 0.4MPa$, hydraulic permeability $k = 1.07 \times 10^{-15}m^4/(N \cdot s)$, fixed charge density $c_0^F = 0.2mEq/ml$, intrinsic Poisson's ratio $v_s = 0.2$, and radius of the specimen $a = 1.5mm$; the gel time $\tau_g = a^2/H_a k$ is of the order 5000s.)

respectively. From these equations, note that the dimensionless applied load is related linearly to the dimensionless lateral expansion. Figure 8 shows the variation with time of the lateral expansion (normalized with respect to the axial displacement multiplied by the aspect ratio a/h) for various external saline concentrations; Fig.9 presents the variation of the applied load with time (normalized with respect to force response of an uncharged solid matrix at equilibrium) for several tissue FCDs. Note that the gel time τ_g for the base case is approximately 5,000s. In both figures, we also show the FEM results from the reference by Sun, Guo, Likhitanichkul, Lai, and Mow (2004) so as to be able to compare with the present short time asymptotic result.

The electrical potential history is given by Eqs. (44a) and (44b) and provided in Fig. 10. At short times, the

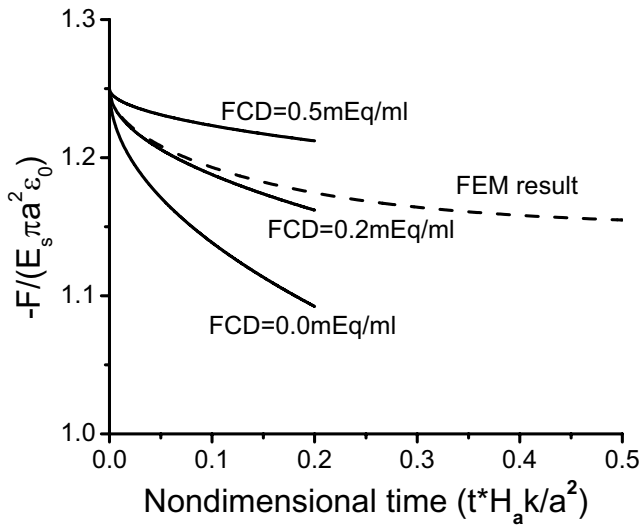


Figure 9 : Predicted short time history of the normalized applied load for a range of initial FCDs in base case, listed in the caption of Fig. 8 (also shown is the numerical FEM full time-dependent result). $\tau_g = a^2/H_a k \sim 5,000s$.

electrical potential in the interior of the tissue remains relatively constant, but in the neighborhood of the edge at $r = a$ there is a boundary layer with a rapidly decreasing potential. Thus, due to this boundary layer, a negative potential gradient exists in the radial direction inside the tissue, which will cause the cations to diffuse relative to the water toward the edge while the anions will move toward the center of tissue.

4 Discussion

The objectives of this paper were to obtain analytic time dependent and equilibrium solutions for the field variables defined in the triphasic theory. A corollary result derived from these solutions is the quantitative relationships between the intrinsic material properties and the apparent measurable mechanical and electromechanical responses from the unconfined compression experiment. Using a perturbation method, the governing PDEs were linearized and solved for the equilibrium results, and using a similarity transformation and introducing a set of non-dimensional parameters, the set of linearized PDEs were transformed into a set of coupled ODEs for the short-time responses of the field variables. From these fundamental governing equations, we found that the entire deformational processes are governed by five

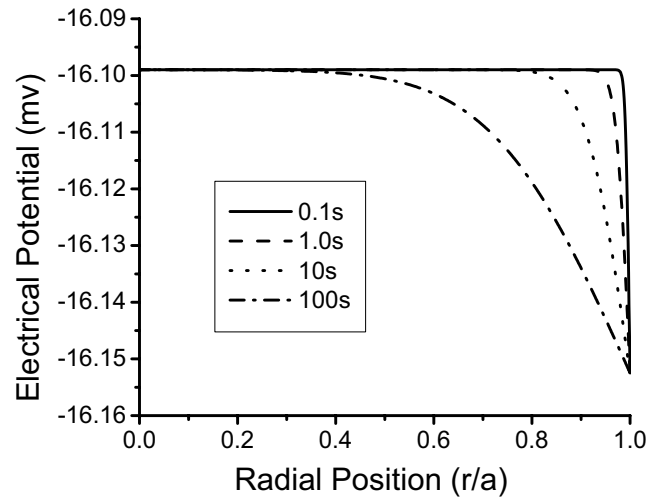


Figure 10 : Predicted electrical potential profile at different times for the base case parameters listed in the caption of Fig. 8.

non-dimensional material parameters v_s , M , f , \hat{D}^+ and \hat{D}^- . These solutions provide simple and analytical expressions for some of the important experimentally measurable quantities commonly found in the literature: lateral expansion, total applied load, and electrical potentials. These measurements provide the necessary data to complete the equations defining coefficients for charged-hydrated tissues. It is important to recall the specific nature of the constitutive assumptions we have used to derive these fundamental results (isotropy, homogeneity, and linearities). Thus within the context of these assumptions regarding tissue composition, material symmetry and equilibrium conditions, we have completely defined the relationships between the intrinsic material properties of such charged-hydrated tissues (and cells), and the experimentally measurable apparent material properties under the strict conditions imposed by this mathematical model of the unconfined compression problem. Although many experimental studies have shown that the external saline concentration may affect both the equilibrium and transient mechanical properties of the articular cartilage, this paper now provides the explicit mathematical relationships defining the dependence of the measured mechanical and chemical properties under unconfined compression, at both short times and steady state, on the external electrolyte, and the intrinsic properties of the tissue.

At equilibrium, there are no gradients of electrochemical potential and thus no movement of water and ions will occur. However, due to the FCD, there is a pressure above the external solution fluid pressure (known as the Donnan osmotic pressure), and an electrical potential difference across the free edge of the specimen at $r = a$. When the osmotic pressure inside the tissue increases, due to increases of the FCD by compression or cellular biosynthesis, or by decreasing c^* of the external solution, an additional compressive stiffness of the tissue will occur; this has been measured by various investigators of the field. The resulting changes of apparent compressive Young's modulus agree well with the experimental results found in reference [Eisenberg and Grodzinsky (1985; 1987)]. To our knowledge, there has been no experimental study on the influence of external ion concentration c^* on the apparent Poisson's ratio. The current analytical results agree well with those recently reported in the reference by Ateshian, Chahine, Basalo and Hung (2004). In this paper, however, we have obtained all the field variables (Tab. 2) including the electrical potential, both transient and at steady state. From our results, we found that all field variables at equilibrium are strongly dependent on the intrinsic Poisson's ratio ν_s and the parameter $\xi (= M/f)$. The former is a measure of the lateral deformation magnitude when there are no fixed charges, and the latter is a measure of the ratio of osmotic pressure change to elastic force change following small deformation. A combination of these two parameters now makes it possible to describe explicitly how osmotic pressure perturbations will affect the measurable apparent properties under unconfined deformation.

The instantaneous deformational response of a triphasic material has been shown to be identical with the biphasic material with equivalent material coefficients [Armstrong, Lai and Mow (1984); Sun, Guo, Likhitanichkul, Lai and Mow (2004)]. At the initial instant, the tissue will expand in the lateral direction without interstitial water flow nor ion transport inside the tissue, except at the very edge where a boundary layer is formed. As the solid matrix recoils and fluid flows efflux occurs, the boundary layer will grow until gradually the deformations penetrates to the center of the sample. At short non-dimensional times following the application of the compression, both the lateral expansion and applied averaged stress will decrease with the square root of time. It is found that the differences between the short time

results and FEM results are less than 5% (with respect to the overall change of lateral expansion or applied load during the stress relaxation process) when the non-dimensional time is less than 0.1. Since the gel diffusion time (*i.e.*, $a^2/(H_a k)$) is about 5000s for the base case, the asymptotic solution agrees very well with the full-time solution for approximately 500s. The kinetics of the stress relaxation provides an additional equation for the determination of the tissue material coefficients. Also, by extrapolating back for $t \rightarrow 0$, our analytical result can be used to calculate the intrinsic shear modulus of the solid matrix, μ_s .

The initial rate of stress relaxation can be estimated from the final solutions, Eqs. (39) and (40), for the lateral expansion and stress relaxation. Generally, the characteristic gel diffusion time of a porous-permeable medium is dependent on the gel diffusivity (*i.e.*, $\tau_g = a^2/(H_a k)$), but for a charged-hydrated medium, it will also depend on many parameters such as the diffusivities of ions and FCD. For instance, for a special case when the diffusivities of the cations and anions are the same, the specific characteristic time is given by:

$$\tau \sim \frac{D^a(1+\xi)}{D^a + H_a k \xi} \left(\frac{1 - \nu_A}{1 - 2\nu_A} \right)^2 \frac{a^2}{H_a k}. \quad (46)$$

Please note that the characteristic time is proportional to the square of the characteristic length of the flow path (a), which agrees with the previous studies on the unconfined compression [Armstrong, Lai and Mow (1984)] and confined compression for the biphasic model [Mow, Kuei, Lai and Armstrong (1980)].

5 Conclusion

In this paper, we have obtained both the short time transient solution and the long time equilibrium solution of a charged-hydrated material subjected to a Heaviside step compressive strain ϵ_0 under the unconfined condition. The triphasic equations were linearized, and the solution was obtained using a regular perturbation method. The exact steady state solution shows that the equilibrium apparent material properties strongly depend on the intrinsic Poisson's ratio and the ratio of the perturbation of osmotic pressure to elastic stress (ξ), and explicit relationships were derived between tissue FCD and the measurable tissue mechanical properties. The short time asymptotic solution enables us to obtain the rapid spatial variations in the various parameters throughout the boundary

layer, as well as to ascertain differences between these values at the boundary and those in the interior of the sample as time progresses. At short times, the lateral expansion and applied load decrease with the square root of time for a considerable fraction of the transient response period and they have been shown to be consistent with the biphasic analysis in earlier study. The results presented in this paper can now be used directly to calculate the intrinsic material properties (*i.e.*, without the effects of the FCD) of the porous-permeable matrix from the experimentally measured (*i.e.*, apparent) material properties, and to quantitatively understand the fundamental nature of the material response.

Acknowledgement: This study was supported by NIH Grants No. AR41913 and AR42850, and the Whitaker Foundation Special Development Award.

Appendix A: Derivation for the Apparent Poisson's Ratio and Young's Modulus

From Eqs. (20)-(24), we have:

$$\delta p = \phi RT \delta c^k, \quad (A1)$$

$$RT \frac{\delta c^+}{c_0^+} + F_c \delta \psi = 0, \quad (A2)$$

$$RT \frac{\delta c^-}{c_0^-} - F_c \delta \psi = 0. \quad (A3)$$

Now by combining Eqs. (A2), (A3) and (13), we obtain:

$$\delta c^k = \frac{c_o^F}{c_0^k} \delta c^F. \quad (A5)$$

To obtain δc^k , Eq.(14) is inserted into the Eq.(A5):

$$\delta c^k = -\frac{(c_o^F)^2}{c_0^k \phi_0^w} \delta e. \quad (A6)$$

Substitution Eq.(A6) into (A1) yields:

$$\delta p = -\frac{\phi RT (c_o^F)^2}{\phi_o^w c_0^k} \delta e. \quad (A7)$$

At the equilibrium, the constitutive equations for the tissue, Eqs. (19a, b, c), become:

$$\delta \sigma_{zz} = -\delta p + \lambda_s \delta e - 2\mu_s \epsilon_0, \quad (A8a)$$

$$\delta \sigma_{rr} = -\delta p + \lambda_s \delta e + 2\mu_s \frac{\partial u_r}{\partial r} = 0, \quad (A8b)$$

$$\delta \sigma_{\theta\theta} = -\delta p + \lambda_s \delta e + 2\mu_s \frac{u_r}{r} = 0. \quad (A8c)$$

In terms of apparent equilibrium Poisson's ratio ν_A , the perturbation of the dilatation δe is given by:

$$\delta e = -\epsilon_0 + \frac{\partial u_r}{\partial r} + \frac{u_r}{r} = (2\nu_A - 1)\epsilon_0. \quad (A9)$$

From Eqs. (A8b), (A8c) and (A9), we have:

$$\frac{\partial u_r}{\partial r} = \frac{u_r}{r} = \nu_A \epsilon_0, \quad (A10)$$

thus by substitution Eqs. (A7), (A9) and (A10) into (A8b) we obtain:

$$\nu_A = \frac{\nu_s + (1 - \nu_s)\xi}{1 + 2(1 - \nu_s)\xi}, \quad (A11)$$

where,

$$\xi = \frac{\phi RT c_0^F c_0^F}{\phi_0^w H_a c_0^k}. \quad (A12)$$

Similarly, the equivalent Young's modulus of the sample at equilibrium may be derived. The component of the (perturbed) stress tensor in the vertical direction is given by:

$$\begin{aligned} \delta \sigma_{zz} &= \delta \sigma_{rr} + (\delta \sigma_{zz} - \delta \sigma_{rr}) = 0 + 2\mu_s(-\epsilon_0 - \nu_A \epsilon_0) \\ &= -2\mu_s(1 + \nu_A)\epsilon_0. \end{aligned} \quad (A13)$$

The apparent equilibrium Young's modulus E_A is equal to the (perturbed) vertical compressive stress divided by the vertical compressive strain ϵ_0

$$E_A = \frac{\delta \sigma_{zz}}{-\epsilon_0} = 2\mu_s(1 + \nu_A) = E_s \frac{1 + \nu_A}{1 + \nu_s}. \quad (A14)$$

Appendix B: The Governing Equations for the Apparent Poisson's Ratio (λ) and Ion Concentration (γ)

Starting with Eqs. (5) and (11), the continuity equations for water and cations can also be written as:

$$\frac{\partial(\phi^w)}{\partial t} + \nabla \cdot (\phi^w \mathbf{v}^w) = 0, \quad (B1)$$

$$\frac{\partial(\phi^w c^+)}{\partial t} + \nabla \cdot (\phi^w c^+ \mathbf{v}^+) = 0. \quad (B2)$$

Combining these two equations, we obtain:

$$\phi^w \frac{\partial c^+}{\partial t} + c^+ \nabla \cdot (\phi^w (\mathbf{v}^+ - \mathbf{v}^w)) + \phi^w \nabla c^+ \cdot \mathbf{v}^+ = 0, \quad (B3)$$

where $\mathbf{v}^+ - \mathbf{v}^w$ is the relative velocity of the cations with respect to water. From the definition of the electrochemical potential of the cations Eq. (9), and Eq. (B3), we obtain:

$$\mathbf{v}^+ - \mathbf{v}^w = -D^+ \left(\frac{\nabla c^+}{c^+} + \frac{F_c}{RT} \nabla \psi \right), \quad (B4)$$

and

$$\begin{aligned} \frac{\partial c^+}{\partial t} + \mathbf{v}^w \cdot \nabla c^+ \\ - \frac{1}{\phi^w} \nabla \cdot \left(\phi^w D^+ \left(\nabla c^+ + \frac{F_c c^+}{RT} \nabla \psi \right) \right) = 0. \end{aligned} \quad (B5a)$$

Similarly, for anions, we have:

$$\begin{aligned} \frac{\partial c^-}{\partial t} + \mathbf{v}^w \cdot \nabla c^- \\ - \frac{1}{\phi^w} \nabla \cdot \left(\phi^w D^- \left(\nabla c^- - \frac{F_c c^-}{RT} \nabla \psi \right) \right) = 0. \end{aligned} \quad (B5b)$$

Eqs. (B5a and B5b) can now be used to directly obtain diffusion transport equations in terms of $c^k = (c^+ + c^-)$ and c^F :

$$\begin{aligned} \frac{\partial c^k}{\partial t} + \mathbf{v}^w \cdot \nabla c^k \\ = \frac{1}{\phi^w} \nabla \cdot \left[\phi^w \frac{(D^+ + D^-)}{2} \left(\nabla c^k + \frac{F_c c^k}{RT} \nabla \psi \right) \right. \\ \left. + \frac{(D^+ - D^-)}{(D^+ + D^-)} \left(\nabla c^F + \frac{F_c c^F}{RT} \nabla \psi \right) \right], \end{aligned} \quad (B6a)$$

and

$$\begin{aligned} \frac{\partial c^F}{\partial t} + \mathbf{v}^w \cdot \nabla c^F \\ = \frac{1}{\phi^w} \nabla \cdot \left[\phi^w \frac{(D^+ + D^-)}{2} \left(\nabla c^F + \frac{F_c c^k}{RT} \nabla \psi \right) \right. \\ \left. + \frac{(D^+ - D^-)}{(D^+ + D^-)} \left(\nabla c^k + \frac{F_c c^F}{RT} \nabla \psi \right) \right]. \end{aligned} \quad (B6b)$$

From Eq.(14), we know that c^F is a function only of the dilatation e under infinitesimal deformation assumption. Therefore, finding the relationship between the electrical

potential ψ in the equations above and dilatation e will reduce the number of independent variables.

By adding Eqs (2), (3) and (4) we obtain:

$$-\rho \nabla \mu^w - \rho^+ \nabla \tilde{\mu}^+ - \rho^- \nabla \tilde{\mu}^- + f_{sw} (\mathbf{v}^s - \mathbf{v}^w) = 0. \quad (B7)$$

For the ideal case when the osmotic coefficient ϕ is 1, and substituting the constitutive equations (8)-(10) into Eq. (B7), we obtain:

$$-\nabla p - F_c c^F \nabla \psi + \frac{1}{k} \mathbf{v}_s = 0. \quad (B8)$$

Taking the divergence of the stress equilibrium equation (7), we have:

$$H_a \nabla^2 e = \nabla^2 p. \quad (B9)$$

Substituting (B9) into (B8), we have the important result:

$$H_a \nabla^2 e = \frac{1}{k} \frac{\partial}{\partial t} e - c^F F_c \nabla^2 \psi. \quad (B10)$$

Using the same regular perturbation sequence as Eq.(18) for the unknowns c^F , c^k , ψ , ϕ^w and e , Eqs. (B6) and (B10) can be written in a cylindrical coordinate system as,

$$\begin{aligned} \frac{\partial \delta c^k}{\partial t} = D^a \frac{1}{r} \frac{\partial}{\partial r} \left(r \frac{\partial \delta c^k}{\partial r} \right) + D^d \frac{1}{r} \frac{\partial}{\partial r} \left(r \frac{\partial \delta c^F}{\partial r} \right) \\ + D^k \frac{F_c c_o^F}{RT} \frac{1}{r} \frac{\partial}{\partial r} \left(r \frac{\partial \delta \psi}{\partial r} \right), \end{aligned} \quad (B11a)$$

$$\begin{aligned} \frac{\partial \delta c^F}{\partial t} = D^a \frac{1}{r} \frac{\partial}{\partial r} \left(r \frac{\partial \delta c^F}{\partial r} \right) + D^d \frac{1}{r} \frac{\partial}{\partial r} \left(r \frac{\partial \delta c^k}{\partial r} \right) \\ + D^F \frac{F_c c_o^F}{RT} \frac{1}{r} \frac{\partial}{\partial r} \left(r \frac{\partial \delta \psi}{\partial r} \right), \end{aligned} \quad (B11b)$$

$$H_a \frac{1}{r} \frac{\partial}{\partial r} (\delta e) = \frac{1}{k} \frac{\partial}{\partial t} \delta e - c_o^F F_c \frac{1}{r} \frac{\partial}{\partial r} (\delta \psi), \quad (B12)$$

where D^a , D^d , D^k and D^F are given by the nomenclature.

Note that the second terms on the left hand side of Eqs. (B6), *i.e.* $\mathbf{v}^w \cdot \nabla c$, have been omitted because such terms are second order in the imposed compressive strain.

If we further introduce the apparent Poisson's ratio λ and dimensionless overall ionic concentration γ as in Eqs. (30) then

$$\delta e = (2\lambda - 1) \varepsilon_0. \quad (B13)$$

From Eqs. (B13) and (14), we obtain:

$$\delta c^F = \frac{c_o^F}{\phi_o^W} \varepsilon_o (1 - 2\lambda). \quad (B14)$$

Finally, Eqs. (30) and (B12) - (B14) can be used to eliminate δc^F , δc^k and $\delta \psi$ from our formulation by substituting these relationships into Eqs. (B11) to yield the two governing PDEs for the two dependent variables:

$$\begin{aligned} \frac{\partial \gamma}{\partial t} = D^a \frac{1}{r} \frac{\partial}{\partial r} \left(r \frac{\partial \gamma}{\partial r} \right) + \frac{D^k}{D^B} \frac{\partial \lambda}{\partial t} \\ - \left(D^k + MD^d \right) \frac{1}{r} \frac{\partial}{\partial r} \left(r \frac{\partial \lambda}{\partial r} \right), \end{aligned} \quad (B15a)$$

$$\begin{aligned} \frac{1}{D^B} \frac{\partial \lambda}{\partial t} = \frac{D^F + MD^a}{D^F + MD^B} \frac{1}{r} \frac{\partial}{\partial r} \left(r \frac{\partial \lambda}{\partial r} \right) \\ - \frac{D^d}{D^F + MD^B} \frac{1}{r} \frac{\partial}{\partial r} \left(r \frac{\partial \gamma}{\partial r} \right). \end{aligned} \quad (B15b)$$

These two equations can readily be rearranged to yield the governing Eqs. (31a and 31b).

References

- Armstrong, C. G.; Lai, W. M.; Mow, V. C.** (1984): An analysis of the unconfined compression of articular cartilage. *J Biomech Eng*, Trans ASME, vol. 106, pp. 165-73.
- Ateshian, G. A.; Soltz, M. A.; Mauck, R. L.; Basalo, I. M.; Hung, C. T.; Lai, W. M.** (2003): The role of osmotic pressure and tension-compression nonlinearity in the frictional response of articular cartilage. *Transport in Porous Media*, vol. 50, pp. 5-33.
- Ateshian, G. A.; Chahine, N. O.; Basalo, I. M.; Hung, C. T.** (2004): The correspondence between equilibrium biphasic and triphasic material properties in mixture models of articular cartilage. *J Biomechanics*, In Press.
- Bachrach, N. M.; Mow, V. C.; Guilak, F.** (1998): Incompressibility of the solid matrix of articular cartilage under high hydrostatic pressures. *J Biomechanics*, vol. 31, pp. 445-51.
- Buschmann, M. D.; Gluzband, Y. A.; Grodzinsky, A. J.; Hunziker, E. B.** (1995): Mechanical compression modulates matrix biosynthesis in chondrocyte/agarose culture. *J Cell Sci*, vol. 108 (Pt 4), pp. 1497-08.
- Carslaw, H. S.; Jaeger, J. C.** (1959): *Conduction of heat in Solids*, 2nd Edition, Ely House, London, UK, Oxford University Press, pp.510.
- Cohen, B.; Lai, W. M.; Mow, V. C.** (1998): A transversely isotropic biphasic model for unconfined compression of growth plate and chondroepiphysis. *J Biomech Eng*, Trans ASME, vol. 120, pp. 491-96.
- Eisenberg, S. R.; Grodzinsky, A. J.** (1985): Swelling of articular cartilage and other connective tissues: electromechanochemical forces. *J Orthop Res*, vol. 3, pp. 148-59.
- Eisenberg, S. R.; Grodzinsky, A. J.** (1987): The kinetics of chemically induced nonequilibrium swelling of articular cartilage and corneal stroma. *J Biomech Eng*, Trans ASME, vol. 109, pp. 79-89.
- Garon, M.; Legare, A.; Guardo, R.; Savard, P.; Buschmann, M. D.** (2002): Streaming potentials maps are spatially resolved indicators of amplitude, frequency and ionic strength dependant responses of articular cartilage to load. *J Biomechanics*, vol. 35, pp. 207-16.
- Gu, W. Y.; Lai, W. M.; Mow, V. C.** (1993): Transport of fluid and ions through a porous-permeable charged-hydrated tissue, and streaming potential data on normal bovine articular cartilage. *J Biomechanics*, vol. 26, pp. 709-23.
- Gu, W. Y.; Lai, W. M.; Mow, V. C.** (1998): A mixture theory for charged-hydrated soft tissues containing multi-electrolytes: passive transport and swelling behaviors. *J Biomech Eng*, Trans ASME, vol. 120, pp. 169-80.
- Heinegard, D.; Bayliss, M.; Lorenzo, P.** (2003): Pathogenesis of structural changes in the osteoarthritic joint. In: K.D. Brandt, M. Doherty, and L.S. Lohmander (ed) *Osteoarthritis*, 2nd Edition, Oxford University Press, U.K., pp. 73-82.
- Huang, C. Y.; Soltz, M. A.; Kopacz, M.; Mow, V. C.; Ateshian, G. A.** (2003): Experimental verification of the roles of intrinsic matrix viscoelasticity and tension-compression nonlinearity in the biphasic response of cartilage. *J Biomech Eng*, Trans ASME, vol. 125, pp. 84-93.
- Jurvelin, J. S.; Buschmann, M. D.; Hunziker, E. B.**

- (1997): Optical and mechanical determination of Poisson's ratio of adult bovine humeral articular cartilage. *J Biomechanics*, vol. 30, pp. 235-41.
- Kim, Y. J.; Sah, R. L.; Grodzinsky, A. J.; Plaas, A. H.; Sandy, J. D.** (1994): Mechanical regulation of cartilage biosynthetic behavior: physical stimuli. *Arch Biochem Biophys*, vol. 311, pp. 1-12.
- Lai, W. M.; Mow, V. C.; Roth, V.** (1981): Effects of nonlinear strain-dependent permeability and rate of compression on the stress behavior of articular cartilage. *J Biomech Eng, Trans ASME*, vol. 103, pp. 61-6.
- Lai, W. M.; Hou, J. S.; Mow, V. C.** (1991): A triphasic theory for the swelling and deformation behaviors of articular cartilage. *J Biomech Eng, Trans ASME*, vol. 113, pp. 245-58.
- Lai, W. M.; Mow, V. C.; Sun, D. D.; Ateshian, G. A.** (2000): On the electric potentials inside a charged soft hydrated biological tissue: streaming potential versus diffusion potential. *J Biomech Eng, Trans ASME*, vol. 122, pp. 336-46.
- Lu, X.; Sun, D. D.; Guo, X. E.; Chen, F. C.; Lai, W. M.; Mow, V. C.** (2004): Indentation Determined Mechano-electrochemical Properties and Fixed Charge Density of Articular Cartilage. *Ann Biomed Eng*, In Press.
- Mankin, H. J.; Mow, V. C.; Buckwalter, J. A.; Iannotti, J. P.; Ratcliffe, A.** (2000): Articular cartilage structure, composition, and function. In: J. A. Buckwalter, T. A. Einhorn, and S. R. Simon (ed) *Orthopaedic Basic Science: Biology and Biomechanics of the Musculoskeletal System*, Rosemont, IL, USA, pp. 443-70.
- Maroudas, A.** (1979): Physicochemical properties of articular cartilage. In: M.A.R. Freeman (ed) *Adult Articular Cartilage*, Kent, UK, pp. 215-90.
- Mow, V. C.; Kuei, S. C.; Lai, W. M.; Armstrong, C. G.** (1980): Biphasic creep and stress relaxation of articular cartilage in compression: Theory and experiments. *J Biomech Eng, Trans ASME*, vol. 102, pp. 73-84.
- Mow, V.C.; Zhu, W.; Lai, W.M.; Hardingham, T.E.; Hughes, C.; Muir, H.** (1989): The influence of link protein stabilization on the viscometric properties of proteoglycan aggregate solutions. *Biochim Biophys Acta*, vol. 112 p. 201-08.
- Mow, V. C.; Ratcliffe, A.; Poole, A. R.** (1992): Cartilage and diarthrodial joints as paradigms for hierarchical materials and structures. *Biomaterials*, vol. 13, pp. 67-97.
- Mow, V. C.; Ateshian, G. A.** (1997): Lubrication and wear of diarthrodial joints. In: V.C. Mow, and W.C. Hayes (ed) *Basic Orthopaedic Biomechanics*, Philadelphia, pp. 273-315.
- Mow, V. C.; Ratcliffe, A.** (1997): Structure and function of articular cartilage and meniscus. In: V. C. Mow, and W. C. Hayes (ed) *Basic Orthopaedic Biomechanics*, Philadelphia, pp. 113-77.
- Mow, V. C.; Ateshian, G. A.; Lai, W. M.; Sun, D. N.; Wang, C. B.; Gu, W. Y.** (1998): Effects of fixed charge density on the stress-relaxation behavior of hydrated soft tissues in confined compression. *Advances in Bioengineering*, ASME, Bioengineering Division, pp. 267-68.
- Mow, V. C.; Wang, C. C.; Hung, C. T.** (1999): The extracellular matrix, interstitial fluid and ions as a mechanical signal transducer in articular cartilage. *Osteoarthritis Cartilage*, vol. 7, pp. 41-58.
- Mow, V. C.; Sun, D. D.; Guo, X. E.; Likhitanichkul, M.; Lai, W. M.** (2002): Fixed negative charges modulate mechanical behavior and electrical signals in articular cartilage under unconfined compression: The triphasic paradigm. In: W Ehlers, J Bluhm (ed) *Porous Media, Proc Tribute to Professor Reint de Boer*, Berlin, pp. 227-47.
- Mow, V. C.; Hung, C. T.** (2003): Mechanical properties of normal and osteoarthritic articular cartilage, and mechano-biology of chondrocytes. In: K. D. Brandt, M. Doherty, and L. S. Lohmander (ed). *Osteoarthritis*, Oxford, UK, pp. 102-12.
- Setton, L. A.; Zhu, W.; Mow, V. C.** (1993): The biphasic poroviscoelastic behavior of articular cartilage: role of the surface zone in governing the compressive behavior. *J Biomechanics*, vol. 26, pp. 581-92.
- Soltz, M. A.; Ateshian, G. A.** (2000): A conewise linear elasticity mixture model for the analysis of tension-compression nonlinearity in articular cartilage. *J Biomech Eng, Trans ASME*, vol. 122, pp. 576-86.
- Spilker, R. L.; Suh, J. K.; Mow, V. C.** (1990): Effects of friction on the unconfined compressive response of articular cartilage: a finite element analysis. *J Biomech Eng, Trans ASME*, vol. 112, pp. 138-46.
- Sun, D. N.; Gu, W. Y.; Guo, X. E.; Lai, W. M.; Mow, V. C.** (1999): A mixed finite element formulation of

triphasic mechano-electrochemical theory for charged, hydrated biological soft tissues. *Int J Num Meth Engng.* pp. 1375-1402.

Sun, D. D.; Mow, V. C.; Lai, W. M.; Guo, X. E. (1999): A triphasic finite element study on articular cartilage behavior in unconfined compression. ASME, Bioengineering Division, p. 111-21.

Sun, D. D.; Guo, X. E.; Likhitpanichkul, M.; Lai, W. M.; Mow, V. C. (2004): The influence of the fixed negative charges on mechanical and electrical behaviors in articular cartilage under unconfined compression. *J Biomech Eng*, Trans ASME, vol. 126, pp. 1-11.

Wong, M.; Ponticello, M.; Kovanen, V.; Jurvelin, J. S. (2000): Volumetric changes of articular cartilage during stress relaxation in unconfined compression. *J Biomechanics*, vol. 33, pp. 1049-54.

Nomenclature

c^* = salt concentration in bath, in mole per unit volume
 c^F = fixed charge density (Eq/unit tissue water volume)
 c^\pm = charge density for cations (+), anions (-) (Eq/tissue water volume)
 D^\pm = diffusivity for cations (+), anions (-)
 e = dilatation of the solid matrix
 \mathbf{E} = infinitesimal deformation tensor of solid matrix
 E_s = (intrinsic) Young's modulus of solid matrix
 E_A = (apparent) equilibrium Young's modulus of the tissue
 F_c = Faraday constant
 $f_{\alpha\beta}$ = drag coefficients between α and β component
 H_a = aggregate modulus of solid matrix
 k = hydraulic permeability
 M_\pm = atomic weight of Na and Cl
 p = interstitial fluid pressure
 R = universal gas constant
 T = absolute temperature
 \mathbf{v}^α = velocity of α -component
 ϵ_0 = compressive axial strain in vertical direction
 λ_s, μ_s = intrinsic Lamé constants of solid matrix
 μ^w = chemical potential per unit mass of water
 $\tilde{\mu}^\pm$ = electrochemical potentials (per mass) for cations (+) and anions (-).

ν_s = (intrinsic) Poisson's ratio of solid matrix
 ν_A = (apparent) equilibrium Poisson's ratio of the tissue
 ϕ = osmotic coefficient
 ϕ^α = volume fraction of α -component
 ρ^α = apparent mass density of α -component
 ρ_T^w = true density of water phase
 σ = stress tensor of mixture

$$D^a = (D^+ + D^-)/2$$

$$D^B = H_a k$$

$$D^d = (D^+ - D^-)/2$$

$$D^k = D^a + (c_o^k/c_o^F)D^d$$

$$D^F = (c_o^k/c_o^F)D^a + D^d$$

$$A = D^a D^F - D^k D^d + M(D^a)^2 - M(D^d)^2$$

$$B_{11} = (D^a D^F + D^a D^B M - D^k D^d) / A$$

$$B_{12} = D^d D^B / A$$

$$B_{21} = M (D^k D^B + D^d D^F + M D^d D^B - D^k D^a) / A$$

$$B_{22} = D^B (D^F + M D^a) / A$$

$$P = \sqrt{(B_{11} - B_{22})^2 + 4B_{12}B_{21}}$$

$$P_1 = (B_{11} - B_{22} + P) / 2$$

$$P_2 = (-B_{11} + B_{22} + P) / 2$$

$$q_1 = (B_{11} + B_{22} + P) / 2$$

$$q_2 = (B_{11} + B_{22} - P) / 2$$

$$\lambda^* = \frac{1}{4(1 - \nu_A)}$$

$$\gamma^* = \frac{1}{4(1 - \nu_A)} - \frac{1}{4(1 - \nu_s)}$$

$$C_3 = \frac{1}{P} \left(\left(\frac{1}{2} - \lambda^* \right) P_1 - \gamma^* B_{12} \right)$$

$$C_4 = \frac{1}{P} \left(\left(\frac{1}{2} - \lambda^* \right) P_2 + \gamma^* B_{12} \right)$$

